Kerbala Journal for Engineering Sciences

https://kjes.uokerbala.edu.iq

Numerical Analysis of Cooling Device Height on Temperature and Airflow Distribution in a Confined Space

Atef Chibani [1,*] , Riad Badji [1]

[1] Research Center in Industrial Technologies CRTI, P.O. Box 64, Cheraga 16014, Algiers, Algeria.

[*]Corresponding author, E-mail: chibaniatef@gmail.com

Received: 28 January 2026; Revised: 17 March 2026; Accepted: 30 March 2026; Published:31March 2026

Abstract

The study makes an important contribution to the research gap that has existed in efforts to maximize energy efficiency and thermal comfort in the indoor environment since it presents an unsteady numerical analysis of the influence of the height of the cooling device on the temperature distribution in an enclosed space. The study employs ANSYS FLUENT 16 to evaluate the influence of the location of the devices on the air velocity, and heat distribution. The findings indicate that a height of 2.4 m for the cooling device is more effective than the other configurations in enhancing the distribution of temperature, and air velocity. It is found that the increase in the height device to 2.4 m at a speed of 2.5 m/s results in an improvement in heat transfer of 0.377% at Point 1 and 0.288% at Point 3. Similarly, the increase in heat transfer at Point 1 and Point 3 at 6.5 m/s is 0.227 % and 0.184 %, respectively. These results prove that height is more influential on the efficiency of heat transfer compared to air conditioning. This paper highlights the importance of the strategic location of cooling systems to enhance their effective use and thermal comfort, thus making contribution towards the sustainable design and operation of structures.

Keywords: Cooling Device; Temperature Distribution; Numerical Analysis**;** ANSYS/FLUENT.

1. Introduction

The growing world concern about energy efficiency has made thermal management in buildings one of the most urgent issues in recent engineering research. Buildings account for a high percentage of the overall energy consumption worldwide, and improving insulation and airflow systems in enclosed areas

https://doi.org/10.63463/kjes1220

has become a pressing priority [1, 2]. It can be stated that the thermal performance of a building envelope directly influences the energy needed to maintain comfortable indoor conditions, and research has consistently shown that an inefficient insulation design results in excessive energy loss [3, 4].

The thermal insulation products play a crucial role in minimizing the heat exchange between the interior and exterior spaces. Both conventional and renewable insulation materials have been introduced, and research has shown that material selection, thickness and positioning have a considerable influence on the total thermal resistance of a building [5,6]. Recent developments include lightweight and thermally superior materials such as flexible syntactic foams, polystyrene/ silica composites, and insulation panels made of bark [7-9].

In addition to material characteristics, the geometrical arrangement of the insulation and cooling devices has a significant impact on the temperature distribution and air circulation patterns in closed spaces. To fulfill the two demands of thermal resistance and structural integrity, high-performance insulation foams with high compressive strength, including BPP foams reinforced with in-situ PTFE fibers have been developed [10]. Moreover, the optimization models of investments and savings have also been used to calculate the economically optimal insulation thickness for external walls, which has proven to be high sensitivity to local climate conditions and energy prices [11,12].

Substantial savings in energy use and carbon emissions have been reported in humid subtropical, and optimum insulation thickness is applied [13]. The use of novel insulation panels is currently being tested from physical and mechanical perspectives to confirm its performance in these fields [14]. When used in combination with insulation strategies, active cooling systems should be well designed to promote equal temperature distribution especially in limited spaces where airflow may become stratified or turbulent.

The position and the height of cooling devices have been stated as significant factors in determining the efficiency of thermal management systems. This has been proven by the experiments and numerical studies that show the placement of vortex generators and air-supply equipment has a strong influence on the heat transfer properties and film cooling efficiency on a flat surface [15]. The analysis of these intricate interactions has become more feasible through computational fluid dynamics (CFD) techniques, which provide detailed information on velocity field, pressure gradient and temperature field, which would otherwise be hard or costly to measure experimentally [16,17].

Numerical analysis has also shown that airflow and thermal stratification produced by jets in the confined space are very sensitive to the shape and height of the air supply unit [18]. Optimization structures and CFD-based frameworks have been developed to optimize HVAC operating parameters to achieve energy-efficient operation, and the findings revealed a significant improvement in indoor thermal comfort and reduction in peak cooling loads [19]. Recent surveys have also pointed to the progress in numerical modeling of indoor airflow and thermal comfort with the increasing role of machine learning-assisted simulations in accelerating the design process [20].

As a sustainable approach, both the life cycle costs of energy systems and their thermal performance should be considered. Design of Energy-efficient office building using life cycle cost has shown that

investment in an optimized cooling and insulation system is economically feasible in tropical cities [21]. Multi-objective algorithms have also demonstrated that building geometry can be systematically optimized to reduce energy loads without violating of architectural and occupancy specifications [22].

The concept of smart control powered by machine learning has also been developed as a useful tool for regulating the energy consumption of environmentally friendly buildings [23]. Surveys about new energy-efficient technologies to develop envelopes, walls, windows, and roofs have emphasized the application of passive and active thermal management to address the already existing best practices [24]. City-scale building energy modeling frameworks that include the effects of microclimate have brought an additional analytical power enabling planners to evaluate energy performance at urban scale building districts [25].

In the design of confined spaces that are exposed to thermal loads are of equal importance as well. Hybrid predictive procedures of construction vibrations caused by the high-speed railway traffic at bridges have shown that vibrational energy transfer may have complex interactions with thermal systems, which emphasizes the importance of multi-physics analysis in the design of building [26]. Explainable artificial intelligence (XAI) methods have been applied to quantify the financial benefits of the energy-efficient building characteristics to offer stakeholders transparent and interpretable assessments of investment returns [27].

Policy frameworks are also important in ensuring that the adoption of energy efficient technologies is faster. Regulatory instruments have been suggested as minimum performance requirements and binding renovation targets to motivate a thermal renovation of the existing building stock, whose validity has been supported by the experience of German-speaking markets [28]. Smart grid methods to construct energy predictors using massive data sets of actual measurements have additionally improved the efficiency of energy modelling tools and made possible more dependable energy forecasting of cooling and heating needs [29]. The use of artificial intelligence to conduct strategic retrofit assessments has shown the effectiveness of prioritized renovation actions to maximize the amount of energy savings per unit of investment in residential buildings [30]. Among emerging responsive building technologies, dynamic photothermal modulation systems using adaptive materials that react to solar irradiance represent a promising future direction, as they provide passive cooling benefits that can complement active HVAC systems [31].

Even though much has been written regarding insulation materials, airflow modeling and energy optimization, the particular effect of the cooling equipment height on the temperature distribution and airflow patterns in enclosed spaces has not been fully explained. These variables have been studied independently or general architectural configurations, without a methodical study of how device elevation changes spatial gradients of temperature and velocity, in an enclosed or semi-enclosed room. This discrepancy inspires the current numerical study, which will seek to avail a detailed exploration of the height of cooling devices on thermal and aerodynamic performance in a confined area, with outcomes on the development of better and more energy-efficient indoor thermal control systems.

2. Numerical procedure

2.1. Physics models

The heating and cooling system considered in the present study measures 0.4 x 0.4 x 1 m which is a realistic model of an actual building system in a confined environment. In order to emphasize the effects of the device height on the thermal and airflow profiles within the computational domain, the analysis was carried out in two different installation heights: 4.2 m and 1.2 m above the floor level. These two heights were strategically selected to portray two extreme cases, one corresponding to a relatively high ceiling location, and the other representing a lower position closer to the occupant.

The schematic diagram (Fig. 1) depicts the computational model of the two positions of the devices and monitored points, which were chosen to measure changes in temperature and velocity change. This arrangement offers a clear basis for evaluating the variations in airflow dynamics between the two configurations and determining which position offers a more uniform and efficient distribution of thermal loads inside the closed space.

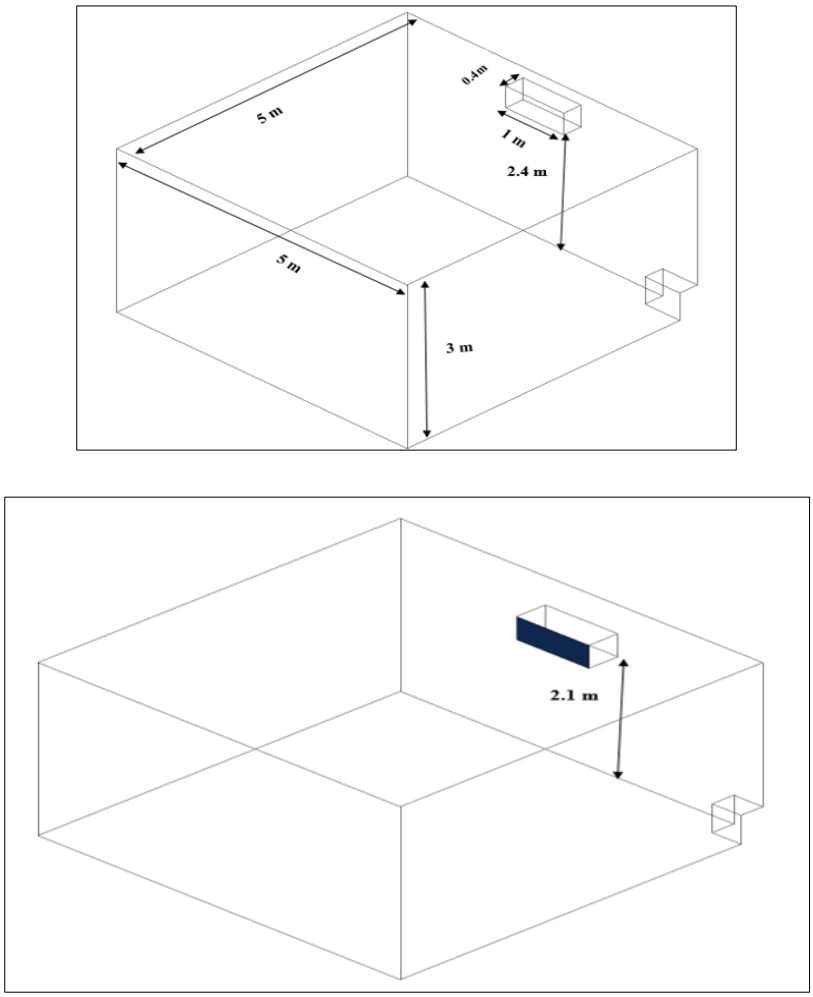

Figure 1. A schematic diagram showing the location of the device and points tested.

2.2. Materials

The working fluid and the main source of thermophysical information used in this study were based on air, as it is commonly used and has a wide range of applications in ventilation, heating, and cooling processes. The choice of air as the working medium is also in line with the real-world conditions of closed spaces where the thermal comfort of occupants and energy performance of HVAC systems directly depend on the thermal and flow behavior of air.

Table (1) summarizes the thermophysical characteristics of air that are essential for ensuring the accuracy and reliability of numerical simulations. These characteristics are density, specific heat capacity, and thermal conductivity which are fundamental parameters in computational fluid dynamics (CFD) for solving the governing equations of fluid flow and heat/mass transfer used in computational work. The model ensures that the simulated outcomes are very close to actual physical processes by integrating these well-proven values and therefore provides confidence in the predicted temperature field and airflow within the computational domain.

Table 1. Thermophysical properties of the materials.

Thermal properties [27]	**Air**
Density [kg/m^3], ρ	1.225
Specific Heat [J/kg K], C_P	1006.43
Thermal Conductivity [W / m K], k	0.0242

According to the manuscript, Figure 2 depicts the computational mesh model that is applied in the numerical simulations in ANSYS FLUENT. The number contains a specific representation of the space that is confined like the geometry of the cooling device and the rest of the domain. After mesh independence test as in Section 2.4, the mesh configuration used was the 52, 342 elements which was chosen to balance a trade off between numerical and computational efficiency so that the eventual temperature and airflow distribution results are no longer dependent on grid resolution.

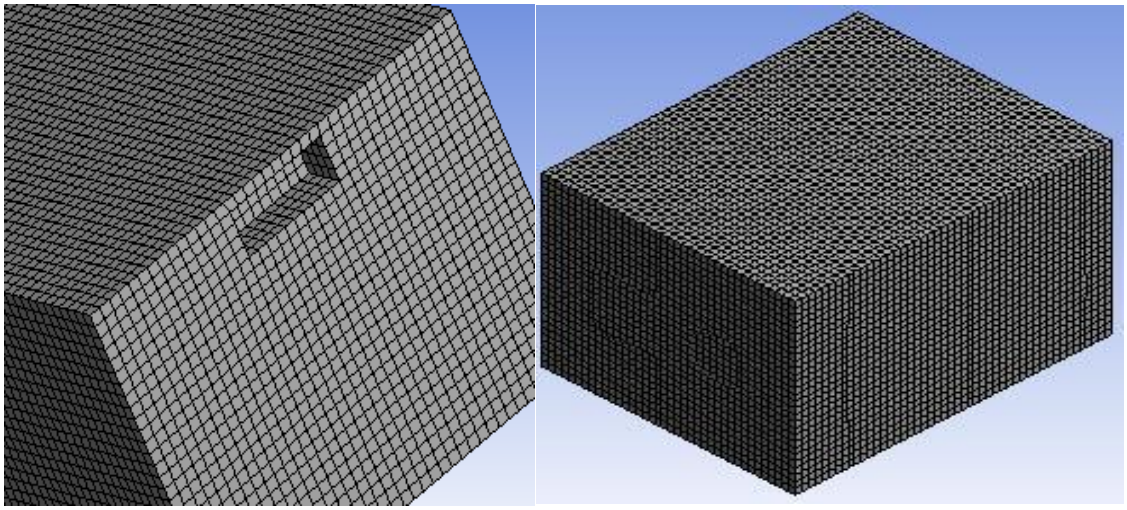

Figure 2. Configuration of the mesh model.

2.4. Grid Independence Test

This part of the study was dedicated to assess the role of mesh density in the phase change behavior for the considered geometrical configuration, with special reference to the principle of mesh independence, which is a fundamental requirement in computational fluid dynamics (CFD) studies. The mesh independence is crucial because it ensures that the numerical result are not artificial effects caused by the mesh refinement, but instead accurately reflect the actual physical phenomena under investigation.

The main aim of this test was to observe the phase change evolution of a heat transfer fluid (HTF) initially subjected to steady flow conditions at 0.2 m/s. In order to do this, four different mesh densities were progressively tested, and the number of elements was 44,567; 47,897; 51, 2342, and 53,342, respectively. There was a consistent thermal and flow behavior of the results at all the tested configurations thus confirming mesh independence.

On the basis of these results, the mesh containing the greatest number of elements (52,342) was chosen for the subsequent numerical simulations since it offered the best trade-off between numerical accuracy and computational efficiency, allowing the most important details of the process of a phase change to be discerned at reasonable computational cost. This result is displayed in Figure 3, which highlights the comparison among the tested meshes and justify the choice of the final mesh.

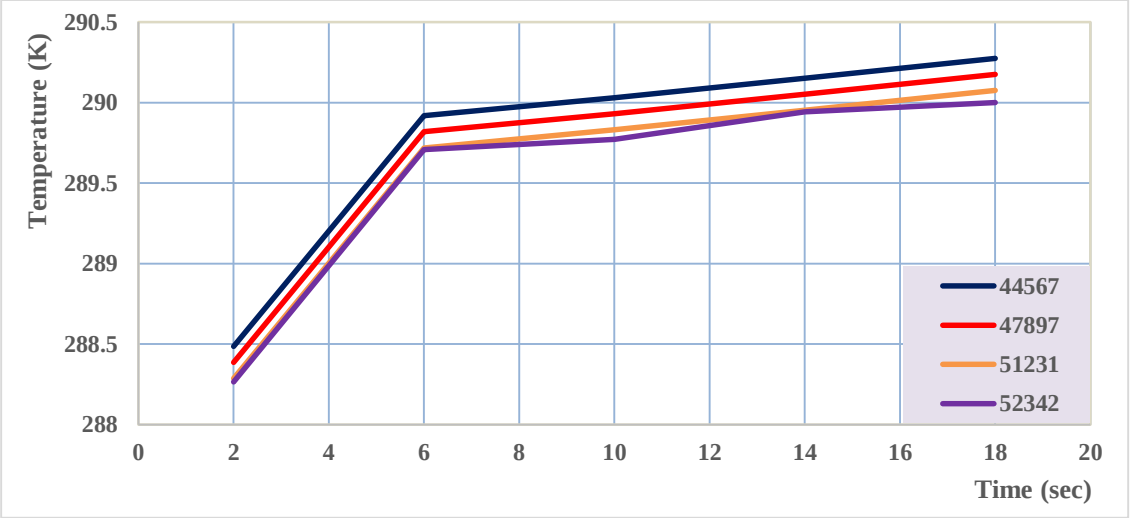

Figure 3. Grid independency test (velocity =2.5 m/s, height (2.1 m)).

2.5. The code validation tests

The validity of the current numerical model is proven by its ability to predict the process of the temperature change throughout the time of the operating conditions in correspondence with the experiment conducted by Zhang et al. [32] (velocity = 2.5 m/s, device height = 2.1 m, monitored at point 1). The two datasets are very close to each other, which proves that the enthalpy porosity formulation together with the turbulence modeling used in the present research were able to achieve the transient behavior of thermal nature and thus confidence is ensured of the simulation framework in future parametric studies regarding the device height and airflow distribution.

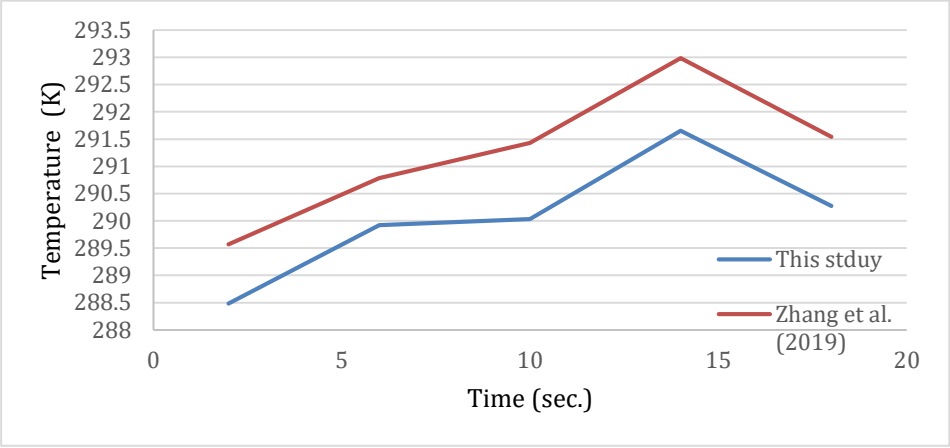

Figure 4. Distinction of the temperature versus operating time for this study against velocity =2.5 m/s, height (2.1 m), point (1), the research [32].

2.6. Numerical Setup and Simulation Parameters

ANSYS/FLUENT 16 was used to conduct the simulations using the enthalpy-porosity formulation, which was utilized to simulate the dynamics of heat transfer and flow. For turbulence modeling, the realizable k-ε model with enhanced wall treatment was chosen because it has been found to be accurate in predicting confined airflow and thermal distributions. The following boundary conditions were applied: velocity inlet with uniform profiles at 0.5, 2.5, 4.5, and 6.5 m/s; at the outlet of the device, pressure outlet on the domain boundaries; and all walls were adiabatic with no-slip. Spatial discretization was performed using a second-order upwind scheme and pressure-velocity coupling was addressed through the SIMPLE algorithm. A time-step of 0.05 seconds was chosen in order to capture transient behavior, and convergence was done when the residuals became smaller than 10^{-6} for the energy equation and 10^{-4} for the continuity and momentum equations.

3. Results and Discussion

To emphasize the relevance of the device height and position in managing the distribution of temperature and air velocity, hence improving indoor thermal comfort for occupants. Two different cases were critically investigated: In case 1, the position of the heating and cooling device was located at 2.1 m, which is a relatively low installation height that restricts the airflow and thermal diffusion inside the space. Compared to the first case, the second one included placing the device at an elevation of 2.4 m, which also allowed the device to cover more area and to distribute cooled or heated air throughout the field. Using these two scenarios, the study aims to offer a better insight of how vertical positioning not only affects the efficiency of heat transfer but also the thermal comfort that is represented within a confined environment.

3.1. Case One: The devise at 2.1 m

To highlight the importance of device height and placement in controlling temperature distribution as well as airflow patterns to achieve a thermally comfortable environment. This study explored two typical scenarios: The first scenario involved placing the heating and cooling apparatus at a height of 2.1 m, which is a relatively low installation that is likely to limit the depth of airflow penetration and thermal diffusion across the enclosed environment. These arrangements frequently lead to local temperature changes and an imbalance in the airflow, which could negatively affect occupant comfort, as shown in Figure 5.

In the second scenario, by contrast, the device was raised to a height of 2.4 m, which facilitated a larger coverage area and a more uniform distribution of conditioned air throughout the area. This increased location enabled the jet of air to propagate further before mixing thus enhancing the uniformity of the temperature field as well as the stability of the velocity distribution which is shown in Figure 6.

Through a logical comparative study of these two settings, the study presents a greater understanding of how the spatial positioning of heating and cooling systems has a direct impact on the efficiency of heat transfer, the energy used, and ultimately, the quality of indoor thermal comfort of constrained spaces. These results were also corroborated by improved thermal homogeneity and greater airflow stability under the elevated device placement, which is further supported in Figure 7. The figure

illustrates a synthesis of the comparative findings, highlighting the practical implications of device height on the overall system performance.

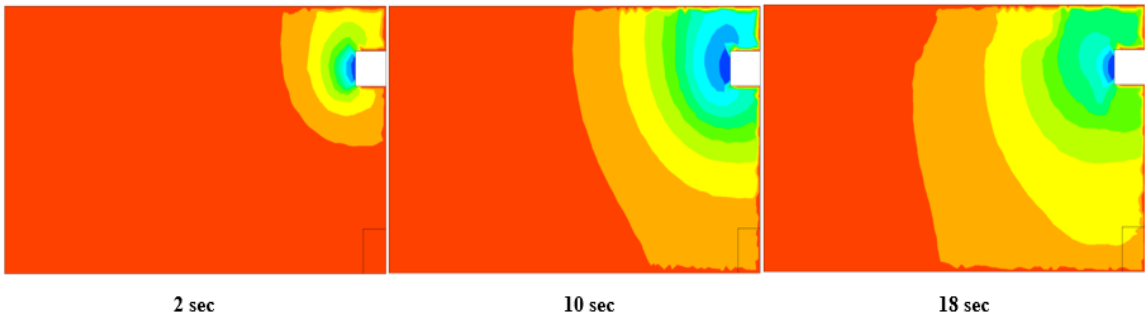

Figure 5. Temperatures at the cell in the velocity (0.5 m/s).

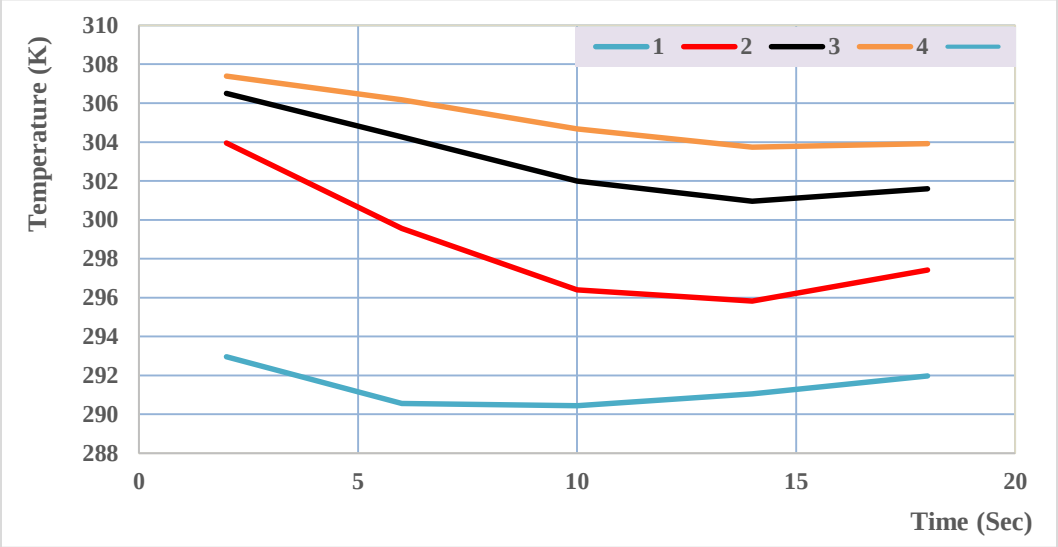

Figure 6. Temperature in point (1,2,3,4) in the velocity (0.5 m/s).

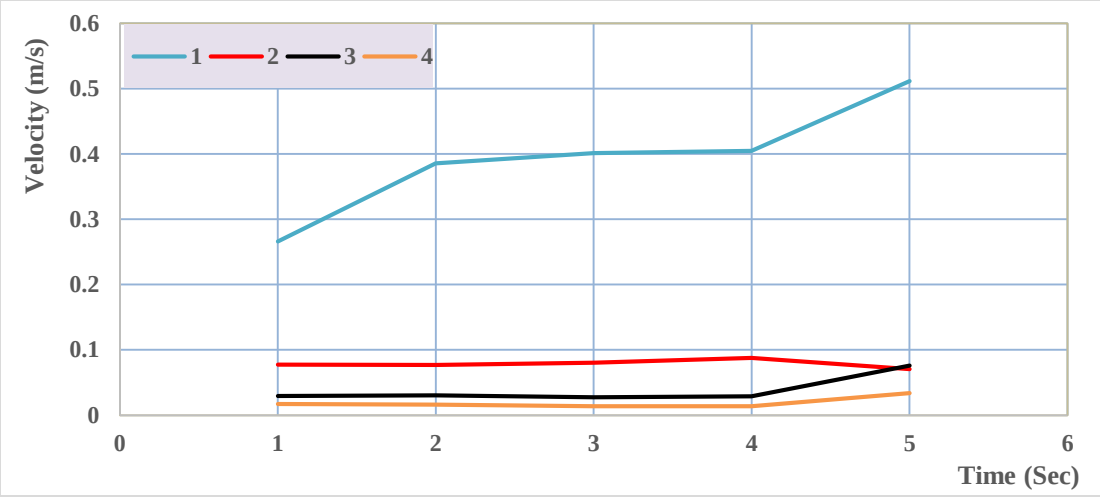

Figure 7. Velocity in points (1,2,3,4) with the velocity (0.5 m/s).

A distribution of temperature in the enclosed space at an inlet air velocity of 2.5 m/s is provided in Figure (8). These findings are clearly shown as that the thermal field is generated at the outlet of the device and slowly diffuses into the room volume, forming thermal layers as the conditioned air interacts with the exterior environment. This gradually decreasing temperature field from the source to the occupied region highlights the impact of momentum and buoyancy effects on the final thermal field.

The further development of the flow leads to the stabilization of temperature both spatially and to more uniform conditions. Figure (9) better captures this trend since it shows the distribution of temperature at the chosen points under the same velocity condition (2.5 m/s). The figure shows that, outside of the initial mixing region, the system approaches a quasi-steady state, which means that the occupants will experience a more uniform thermal environment with fewer local fluctuations.

In addition to these observations, Figure (10) shows the corresponding air velocity distribution at 2.5 m/s. The analysis indicates that it takes the airflow a comparatively short period of time to stabilize following its release out of the device and then attain a relatively constant magnitude of the velocity in a wide segment of the domain. This stability is important in maintaining an efficient mixing as well as thermal comfort because it reducess tagnation zones and enhances the uniform distribution of conditioned air.

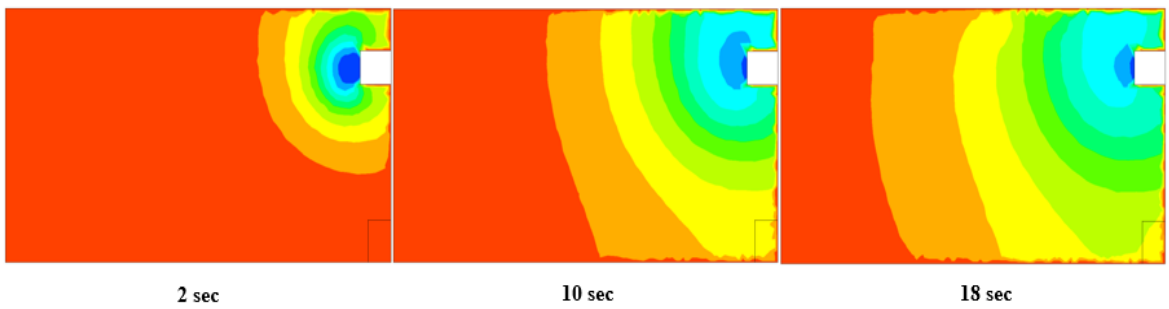

Figure 8. Temperatures at the cell in the velocity (2.5 m/s).

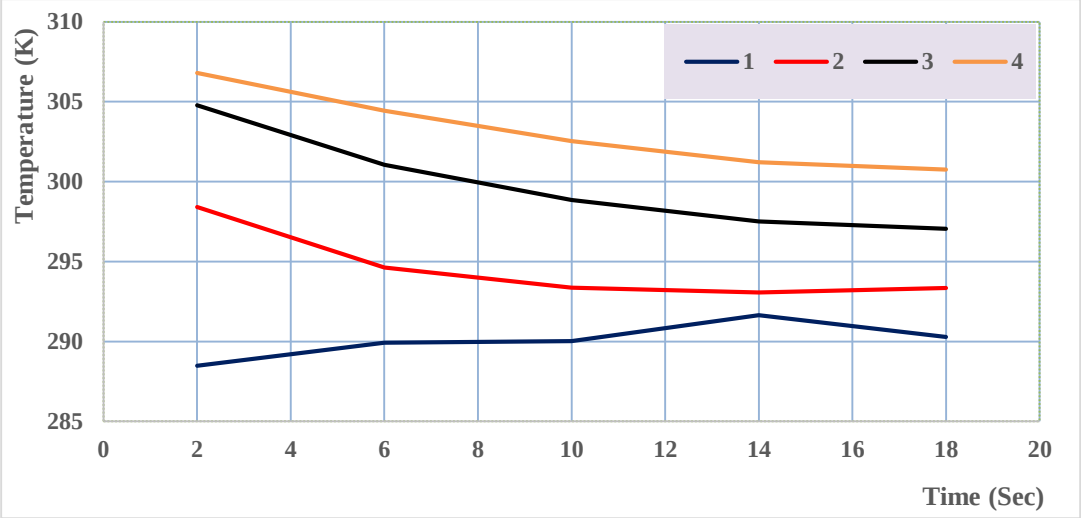

Figure 9. Temperature in point (1,2,3,4) in the velocity (2.5 m/s)

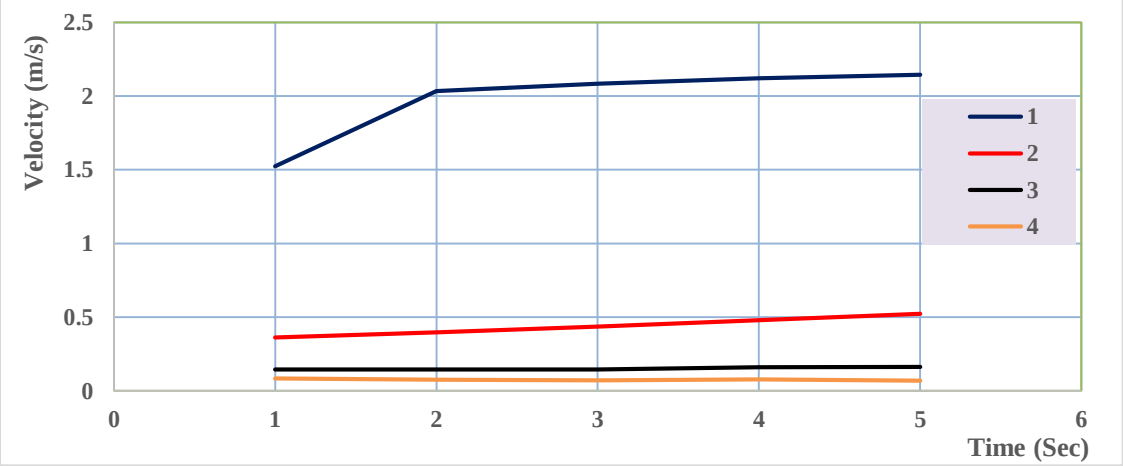

Figure 10. Velocity in points (1,2,3,4) with a velocity (2.5 m/s).

Figure (11) shows the temperature distribution in the entire domain at an inlet velocity of 4.5 m/s. The contours show that the thermal field is formed at the device outlet and extends further into the space,with a distinct downward curve as the conditioned air mixes with the rest of the surroundings. This means that the greater the inlet velocity, the greater the depth of penetration of the air, the greater the effect of temperature can be felt in other parts of the enclosure.

The temperature starts to become homogeneous as the flow progresses and the thermal comfort conditions become more uniform. This is shown in Figure (12), which shows the temperature distribution at the selected monitoring points, under which the same velocity condition (4.5 m/s) is maintained. The figure shows how localized gradients decrease as the system reaches thermal equilibrium, a fact which enhances the overall homogeneity of the thermal field in the occupied zone.

Meanwhile, Figure (13) represents the velocity distribution of the airflow at 4.5 m/s, as well as the location at which the velocity reaches stability and sustains a relatively constant value soon after leaving the apparatus. The high speed flow is necessary to maintain consistent circulation patterns contributing to minimal dead zones and effective mixing of conditioned air, thus highlighting the ability of higher inlet velocity flow to achieve this rapid stabilization.

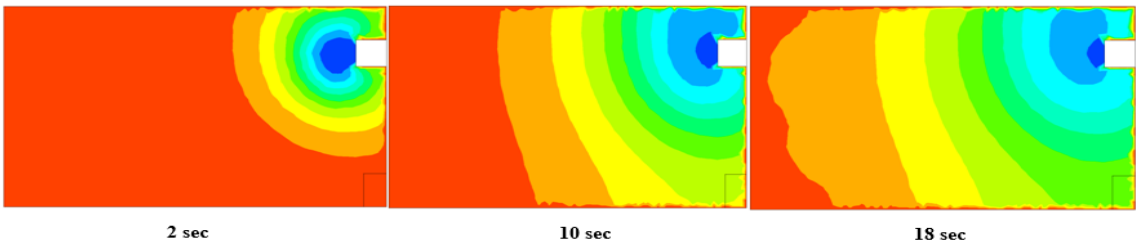

Figure 11. Temperatures at the cell in the velocity (4.5 m/s).

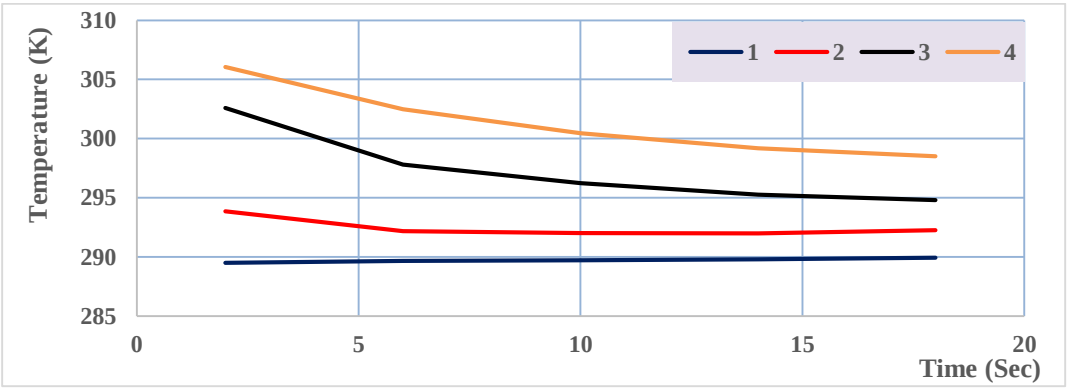

Figure 12. Temperature in point (1,2,3,4) in the velocity (4.5 m/s).

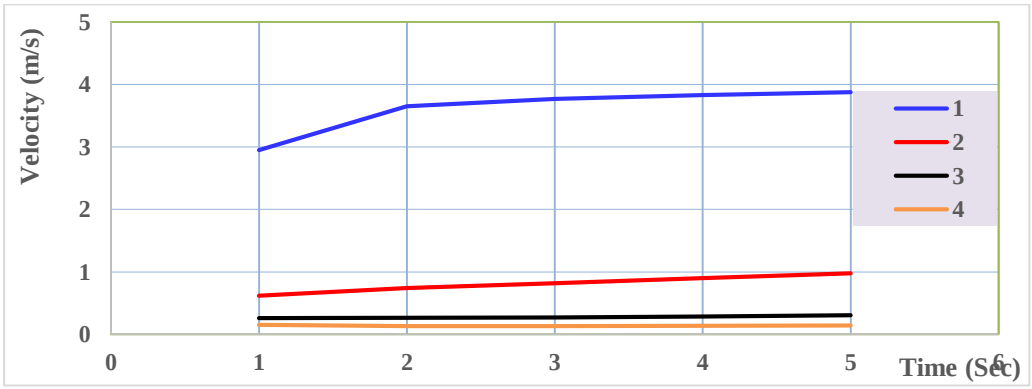

Figure 13. Velocity at points (1,2,3,4) in the velocity (4.5 m/s).

Figure (14) shows the distribution of temperature in the domain with an inlet velocity of 6.5 m/s. In this increased velocity, the thermal field originates at the level of the device and then gradually decreases and diffuses all through the space. This behavior shows that the increased jet momentum increases the

vertical and horizontal penetration, allowing the conditioned air can penetrate a larger area of the domain compared with lower velociy case.

The thermal field becomes more uniform and the temperature distributions also become more uniform as the flow develops. Figure (15) clearly shows this trend by presenting the temperature distribution at the selected monitoring points at the same inlet velocity (6.5 m/s). The figure indicates the capacity of the system to reduce local variations since the air mixes rapidly and approaches a quasi-steady temperature distribution across the observed zones.

Complementary information is given in Figure (16) which shows the air velocity distribution at 6.5 m/s along with the regions where velocity stabilizes and attains a comparatively constant profile soon after flow initiation. The findings affirm the fact that at such a high rate, the movement of the air is stabilized very quickly, resulting in strong circulation and effective air mixing throughout the space.

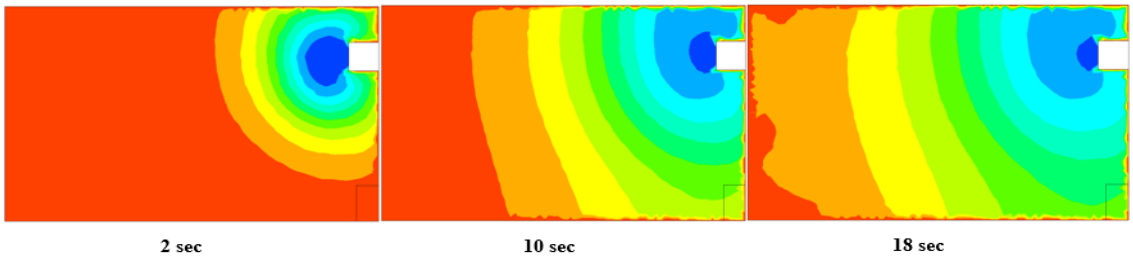

Figure 14. Temperatures at the cell in the velocity (6.5 m/s).

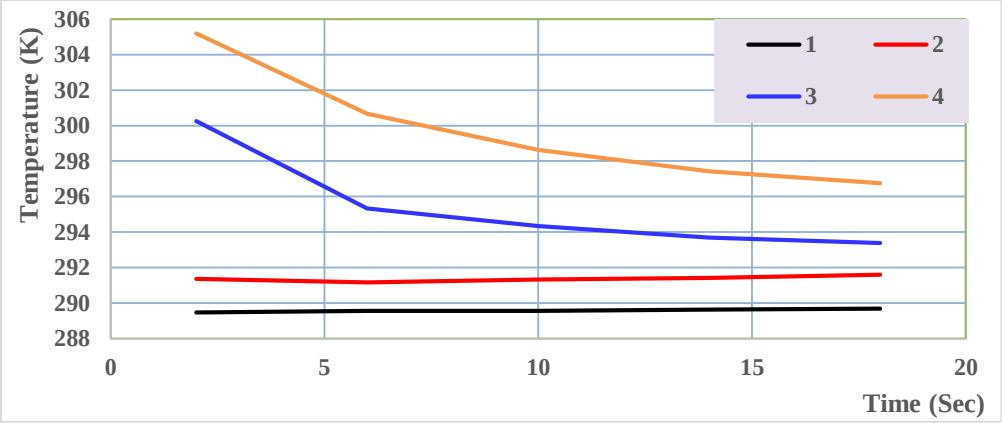

Figure 15. Temperature in point (1,2,3,4) in the velocity (6.5 m/s).

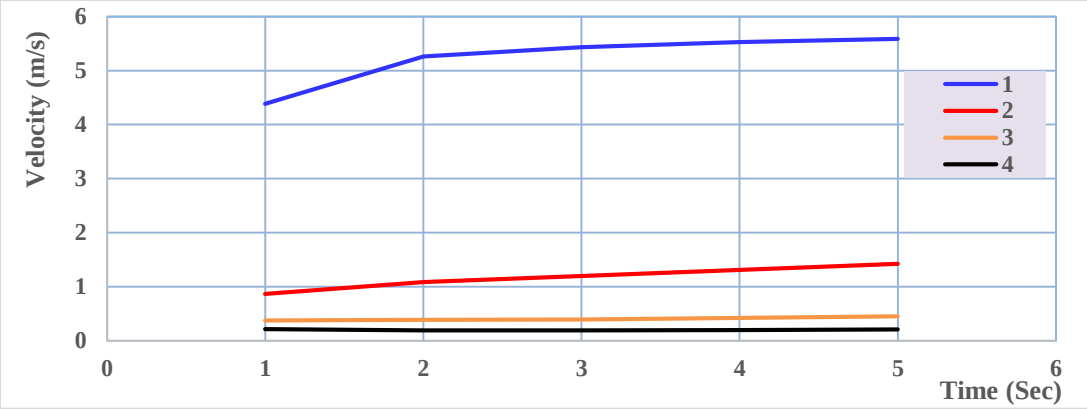

Figure 16. Velocity in points (1,2,3,4) at a velocity (6.5 m/s).

3.2. Case Two: The device at 2.4 m

The height of the device in this case 2.4 m was chosen to be analyzed in detail since it was noted that installation at this height allows the airflow to reach the whole domain effectively. This layout significantly affects the rate of air circulation and the level of thermal diffusion which are important elements in defining the thermal comfort of occupants. It was determined that the airflow spread in an almost homogeneous way throughout the space, and that it followed a semi-straight path starting at the top and occupying all the space with minimal stagnation areas.

Figure (17) below shows the resulting temperature field within the domain at various inlet velocities. The contours clearly depict how the temperature first increases near the level of the device then decreases into the occupied area and then expands to occupy the entire space. Such behavior reveals how effectively the installation height of 2.4 m provides full thermal coverage.

To further explain the process of stabilization, Figure (18) indicates the temperature distribution at some of the monitoring points for the velocities tested. This means that the temperature field stabilizes slowly over time, and gradually become more uniform with few local variations, thereby improving occupant comfort.

Figure (19) offers complementary information since it illustrates the air velocity distribution of the velocity at the analyzed inlet speeds. The figure indicates the location where airflow can stabilize, and maintain itself, a process that takes place at a relatively rapid rate once it leaves the device. Such quick stabilization guarantees the effective mixing of air and increases the capacity of the system to remain consistent in the patterns of circulation in the space.

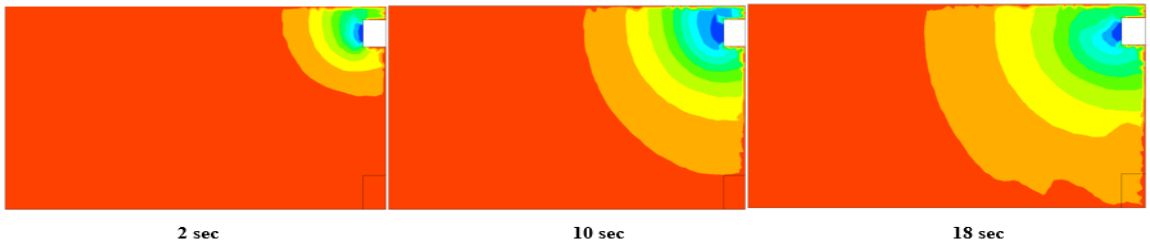

Figure 17. Temperatures at the cell in the velocity (0.5 m/s).

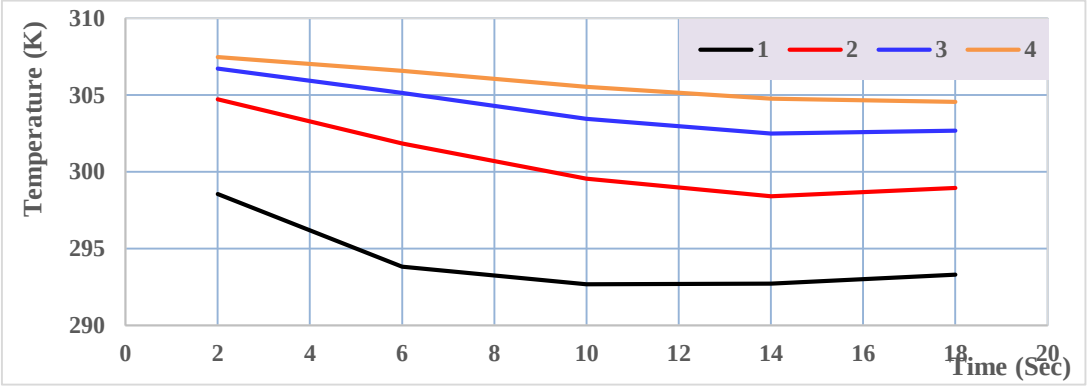

Figure 18. Temperature in point (1,2,3,4) in the velocity (0.5 m/s).

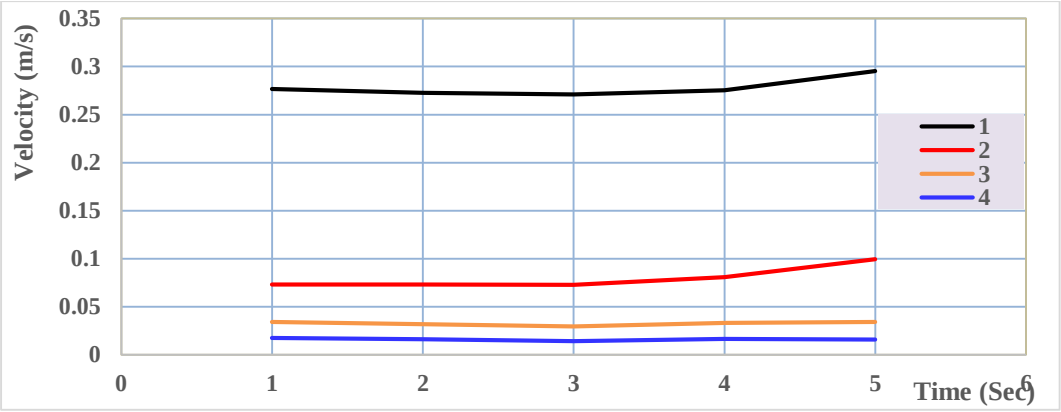

Figure 19. Velocity in points (1,2,3,4) with a velocity (0.5 m/s).

Figure (20) shows the temperature distribution in the domain at various inlet velocities. The outcomes show that the trend is similar, the thermal field at the beginning approaches the same level as the device but then extend toward the occupied zone and finally disperses to occupy the whole space. This development provides emphasizes the strong effect of airflow momentum on the vertical and horizontal distribution of temperature within the domain.

Additional information is given in Figure (21) which shows the distribution of temperature at the chosen monitoring points under different conditions of velocity. The data point to the fact that once the propagation process is completed, the temperature field begins to stabilize, which guarantees greater uniformity throughout the area, as well as fewer local variations, which may otherwise have a significant impact on the well-being of occupants.

Besides that, Figure (22) illustrates the air velocity distribution for the inlets analyzed in terms of inlet speed, and the point where the airflow stabilizes and attains a constant profile nearly instantaneously at the beginning of the process. This quick stabilization is imperative for promoting regular circulation patterns, effective mixing and a more balanced thermal environment in the space.

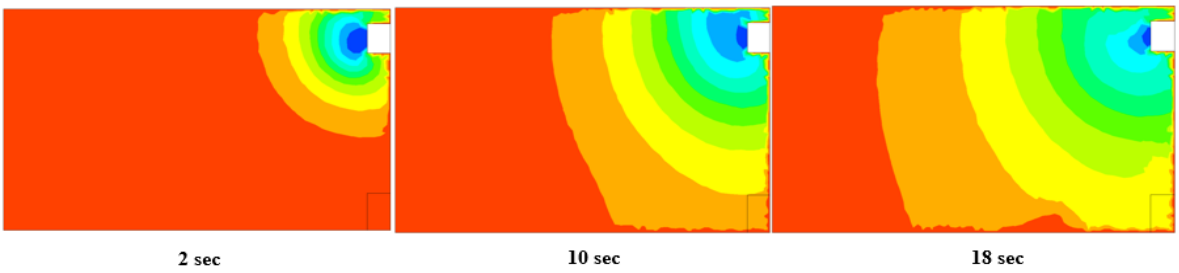

Figure 20. Temperatures at the cell in the velocity (2.5 m/s).

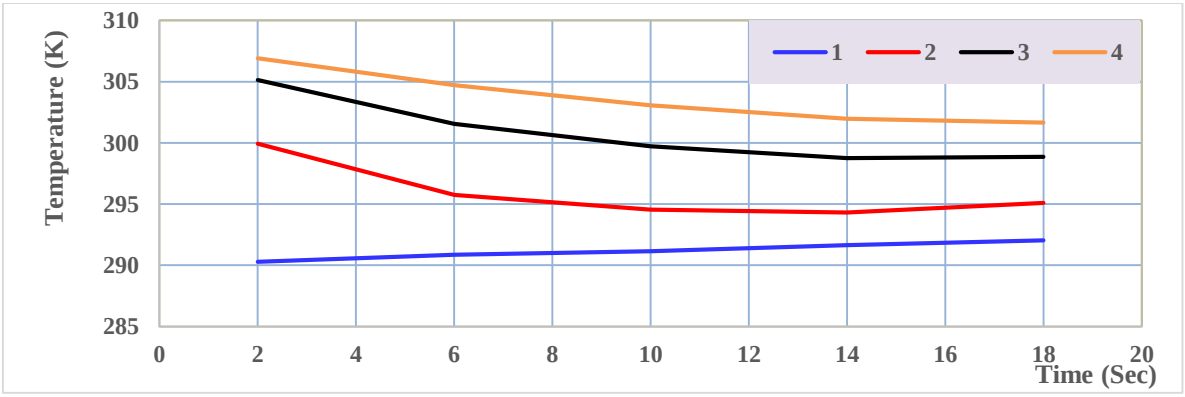

Figure 21. Temperature in point (1,2,3,4) in the velocity (2.5 m/s).

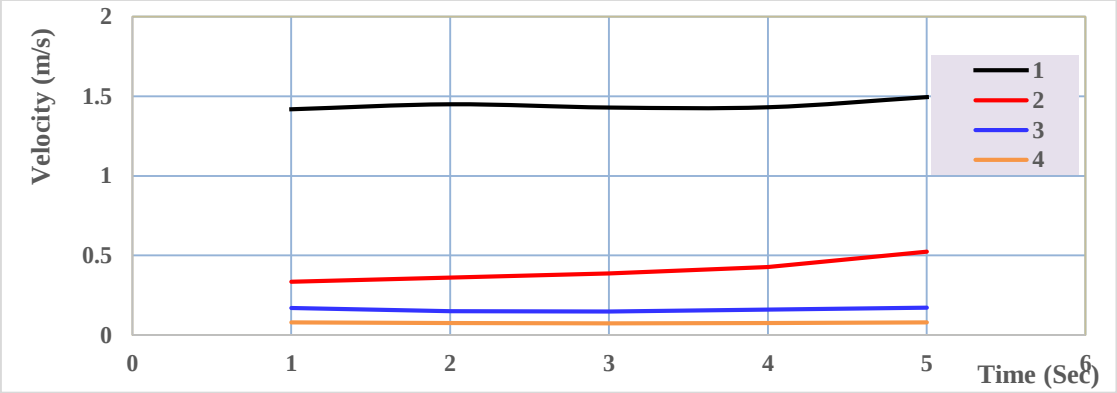

Figure 22. Velocity in point (1,2,3,4) with a velocity (2.5 m/s).

Figure (23) shows the temperature field across the space for the analyzed inlet velocities. The findings reveal an interesting trend in which the initial stage of the thermal field takes up the height of the device followed by a gradual decrease into the occupied area and finally spreads to fill the entire space. This behavior indicates that the system is able to reach full coverage and good mixing of heat with different rates of airflow.

To give a better picture of the stabilization process, Figure (24) depicts the temperature distribution at specific monitoring points for the same range of inlet velocities. These results show that, once a certain period of adjustment is completed, the temperature becomes more stable and this is an indication that a more homogeneous thermal field is formed throughout the domain. This kind of stabilization is essential for reducing the local hot or cold spots that may have an undesirable impact on user comfort.

Additional information on the behavior of the flow are given in Figure (25) that shows velocity distribution at the inlet speeds examined. The figure marks the instability of the airflow, where it becomes stable and maintains a constant pattern, which happens very soon after the air has left the device. This has been achieved through rapid stabilization which provides strong and stable circulation that enhances mixing and the uniformity of the temperature throughout the space.

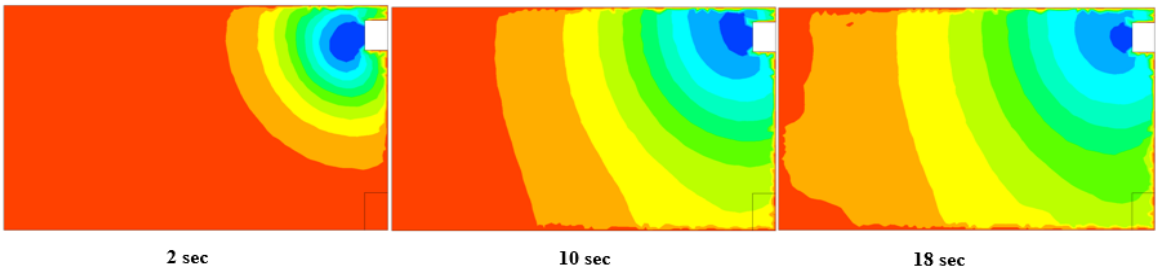

Figure 23. Temperatures at the cell in the velocity (4.5 m/s).

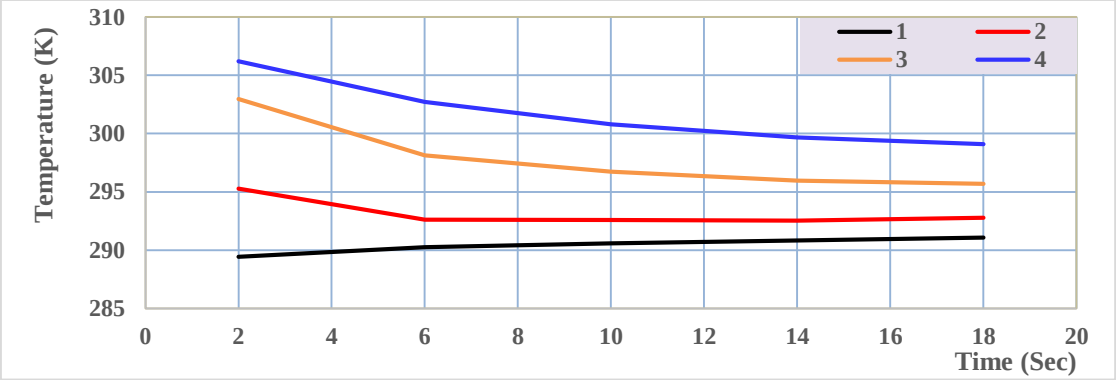

Figure 24. Temperature at points (1,2,3,4) in the velocity (4.5 m/s).

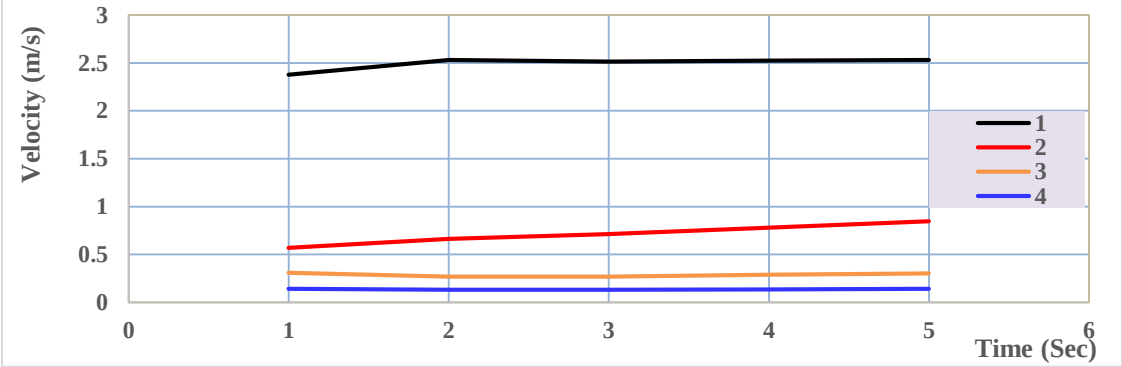

Figure 25. Velocity at points (1,2,3,4) with velocity (4.5 m/s).

Figure (26) shows the temperature distribution within the domain at the inlet velocities studied. The contours portray a transient process whereby the thermal field initially increases to the height of the device, and subsequently extend toward, it falls into the occupied zone, eventually spreading throughout the space. This behavior highlights the combined effect of jet momentum and buoyancy in driving the spread of conditioned air within the enclosure.

As an additional indication, Figure (27) shows the temperature at the selected monitoring points at the various velocities. The findings confirm that the temperature field stabilizes after the first transitional period and hence a more homogeneous thermal environment is developed. This type of stabilization decreases local temperature differences, and in this way, the general state of comfort is enhanced throughout the space.

Simultaneously, Figure (28) shows the airflow velocity distribution at the investigated inlet speeds, together with the point where the velocity reaches a steady value and remains stable shortly after leaving the device. This quick stabilization demonstrates the effectiveness of the airflow in creating stable circulation patterns and hence proper mixing and uniform thermal coverage in the domain.

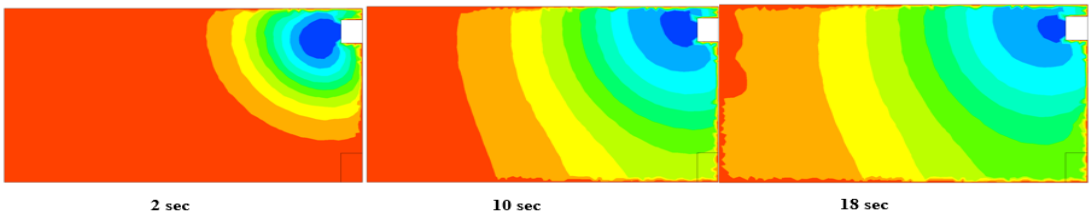

Figure 26. Temperatures at the cell in the velocity (6.5 m/s).

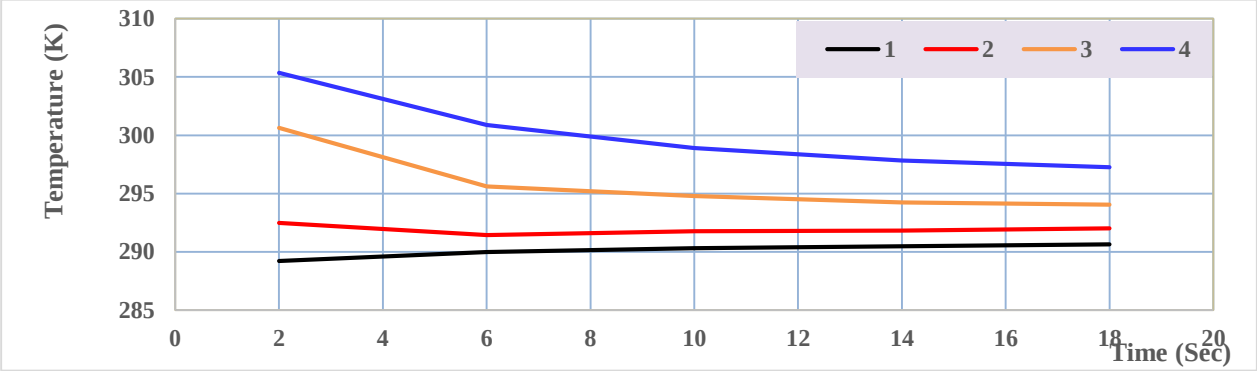

Figure 27. Temperature in point (1,2,3,4) in the velocity (6.5 m/s).

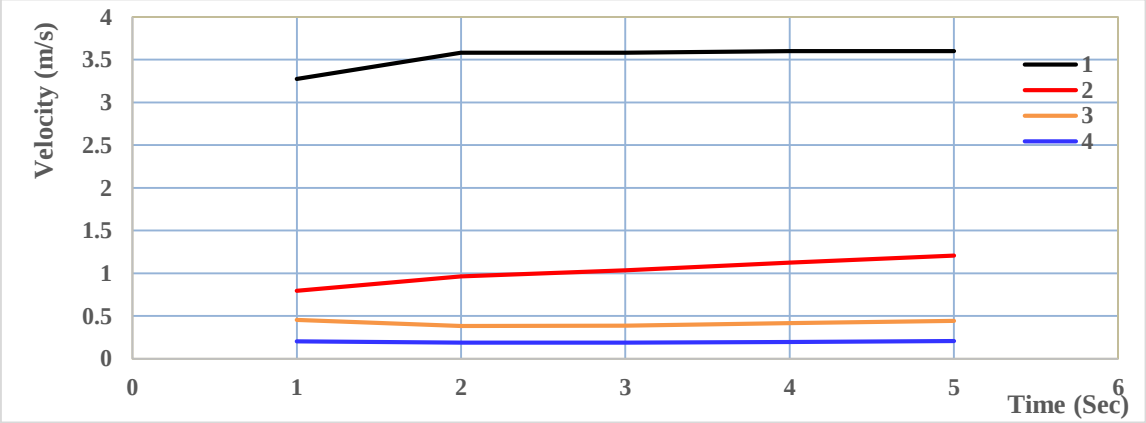

Figure 28. Velocity at point (1,2,3,4) in the velocity (6.5 m/s).

3.3. Comparisons of All Cases

In the comparison of the cases investigated to identify the most appropriate installation height, one can conclude that the optimal installation height for the heating and cooling equipment is 2.4 m. The distribution of airflow and temperature is more desirable at this height since the device encompasses a greater portion of the area when it is installed higher, and the air has a greater distance to travel before it is discharged. This has the effect of enhancing mixing, increasing coverage, and eventually creating a more homogeneous indoor climate.

Figure (29) and (30) demonstrate that the comparative analysis can distinguish the differences in temperature distribution between both heights under the investigated velocities. The findings indicate obviously that the 2.4 m configuration provides more effective temperature distribution throughout the space. Figure (31-34) also supports this observation by demonstrating the temperature behavior at the monitoring points (1) and (3). The data support the statement that the elevated position (2.4 m) improves uniformity of temperatures and minimizes local discrepancies as opposed to the low-height configuration.

As shown in Figures (35-38), the velocity distribution at the studied locations shows that air spreads into points (1) and (3), and it is more efficient at the higher installation height. The findings highlight the fact that the larger the height of the device, the faster it will transfer heat and enhance the efficiency of the process in general.

These conclusions are supported by quantitative analysis. At point (1), the increase in heat transfer with an increase of device height at a velocity of 2.5 m/s was 0.377 % and at point (3) it was 0.288 percent. The gain in heat transfer at point (1) at a higher velocity of 6.5 m/s was 0.227 % and at point (3) it was 0.184 %. These percentages might not seem impressive, but they show a steady improvement in the thermal performance that can be explained by the rise in the installation height.

Although the theoretical heat transfer gains of less than 0.5 % may seem small in numerical terms, their practical implications are for long-term building energy performance and thermal comfort are significant. Given that heating, ventilation, and air conditioning (HVAC) systems operate over long periods, even modest gains in efficiency in any given marginal area can be converted into meaningful energy savings when multiplied by numerous cooling cycles or extended periods of operation or large building area. In addition, the temperature uniformity improvements that are observed due to the better distribution of airflow to optimal device height directly contribute to a decrease in local temperature differences, and as a result, to the reduction of occupant discomfort and the necessity to adjust the system on a regular basis. Therefore, the usefulness of the results is not confined to the extent of the heat transfer enhancement, but rather to the broader benefits of improved thermal homogeneity and system responsiveness, which together contribute to more sustainable and comfortable indoor settings.

The high device height (2.4 m) enables the supply jet to penetrate further into the space before the forces of buoyancy take over, hence, increasing the vertical mixing and decreasing the thermal stratification. It is implied that the enhanced thermal uniformity of this height is due to greater entrainment of ambient air by the jet, the reduced attachment of the jet to the ceiling, the formation of a larger recirculation zone and the improved distribution of conditioned air within the occupied space. Not only is this interpretation able to discuss the observed 0.377% increase in heat transfer at lower velocities but it also explains why height changes tend to affect the thermal field to a greater extent than only velocity change alone- a fact that suggests the significance of proper device placement in maximizing both thermal comfort and energy efficiency.

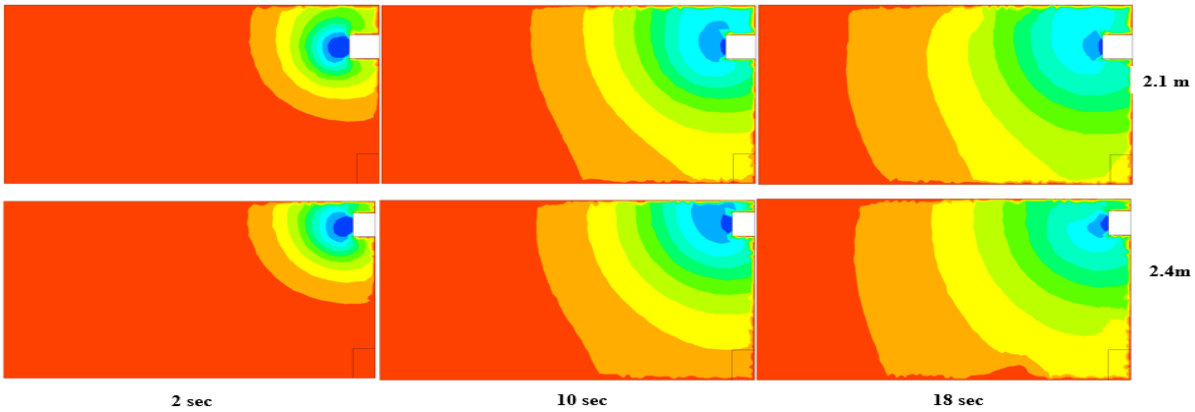

Figure 29. Comparison of all cases (temperatures in the velocity (2.5)).

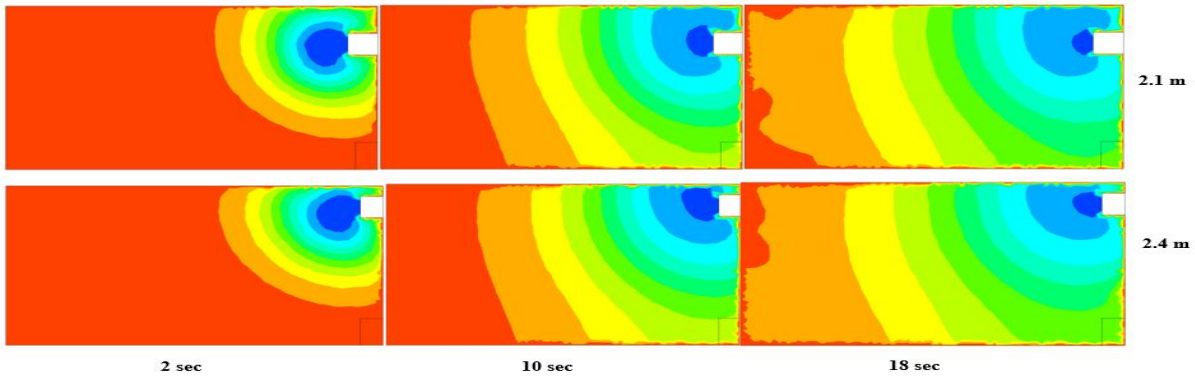

Figure 30. Comparison of all cases (temperatures in the velocity (6.5 m/s).

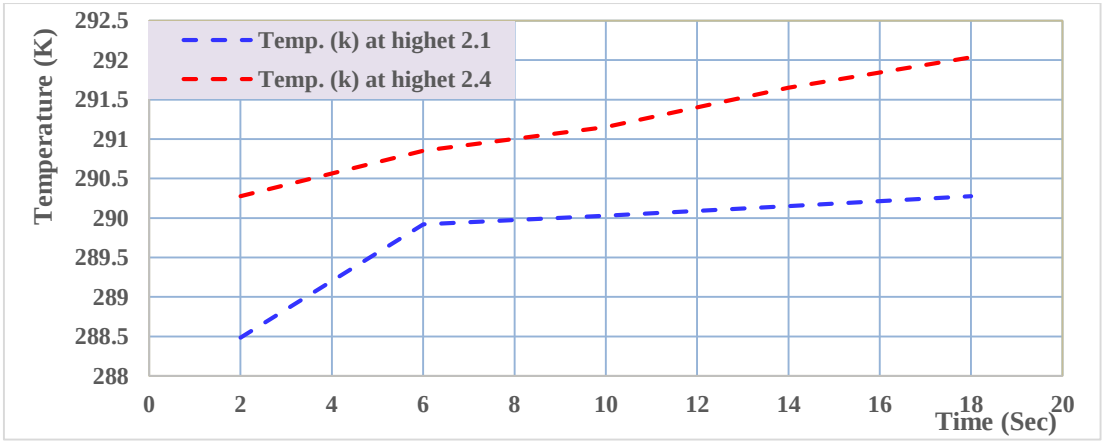

Figure 31. Comparison of all cases (temperature in point (1) in the velocity (2.5 m/s)).

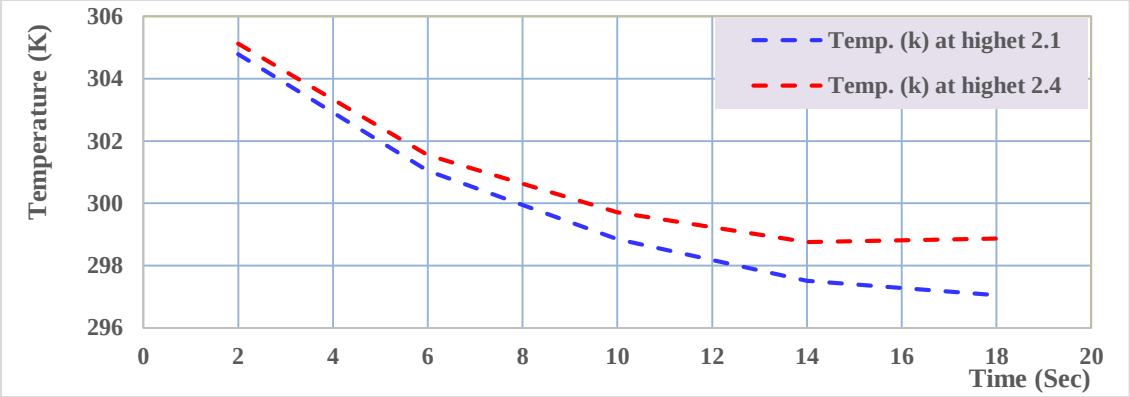

Figure 32. Comparison of all cases (temperature in point (3) in the velocity (2.5 m/s)).

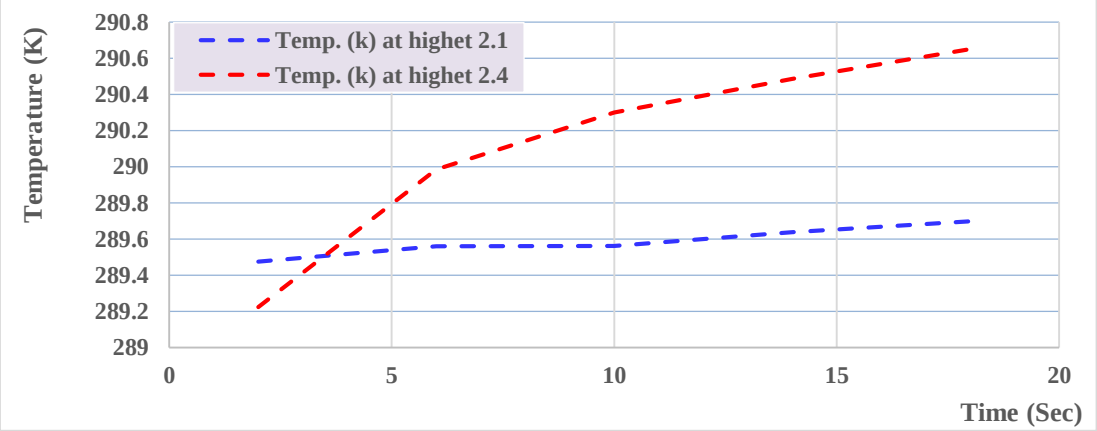

Figure 33. Comparison of all cases (temperature in point (1) in the velocity (6.5 m/s)).

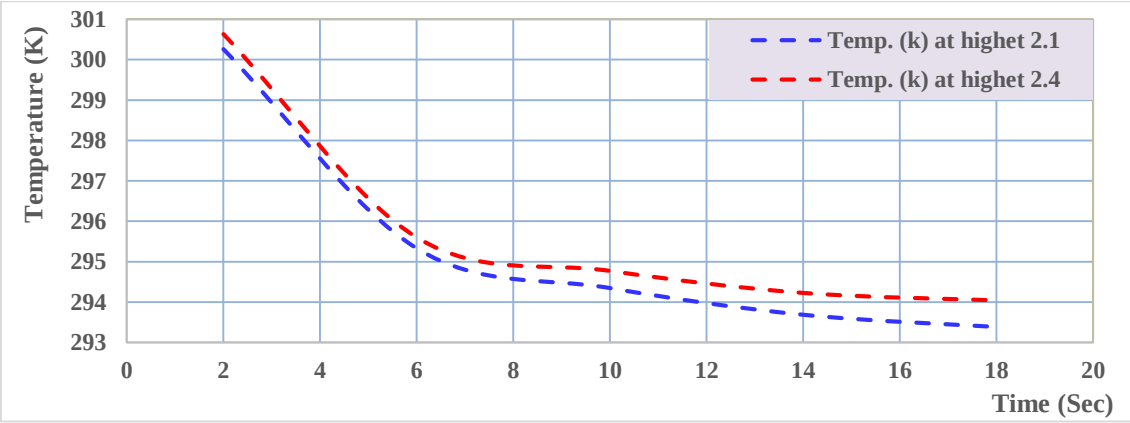

Figure 34. Comparison of all cases (temperature in point (3) in the velocity (6.5 m/s)).

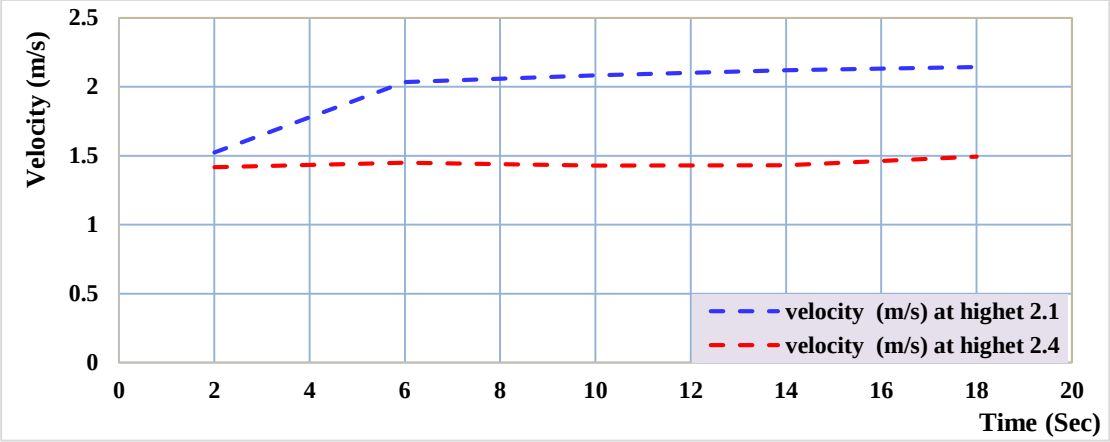

Figure 35. Comparison of all cases (velocity in point (1) in the velocity (2.5 m/s)).

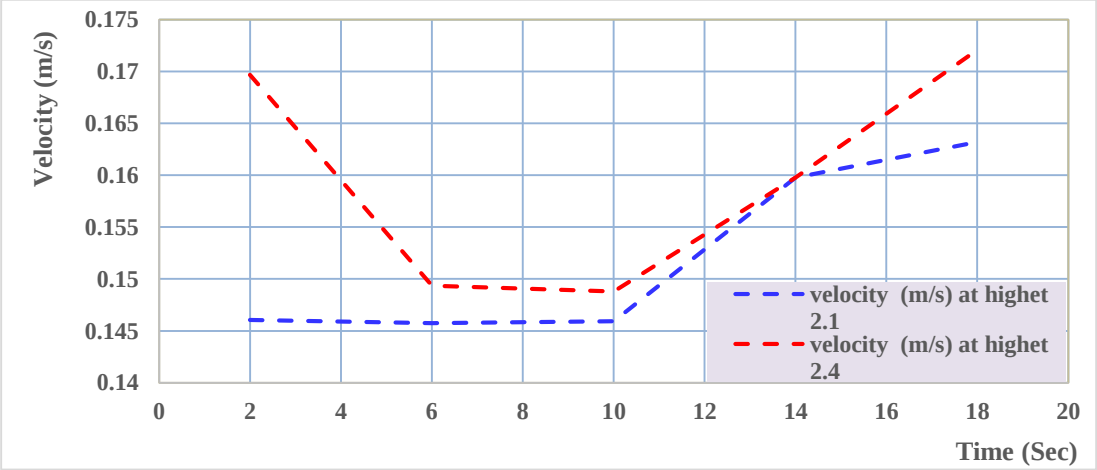

Figure 36. Comparison of all cases (velocity in point (1) in the velocity (6.5 m/s)).

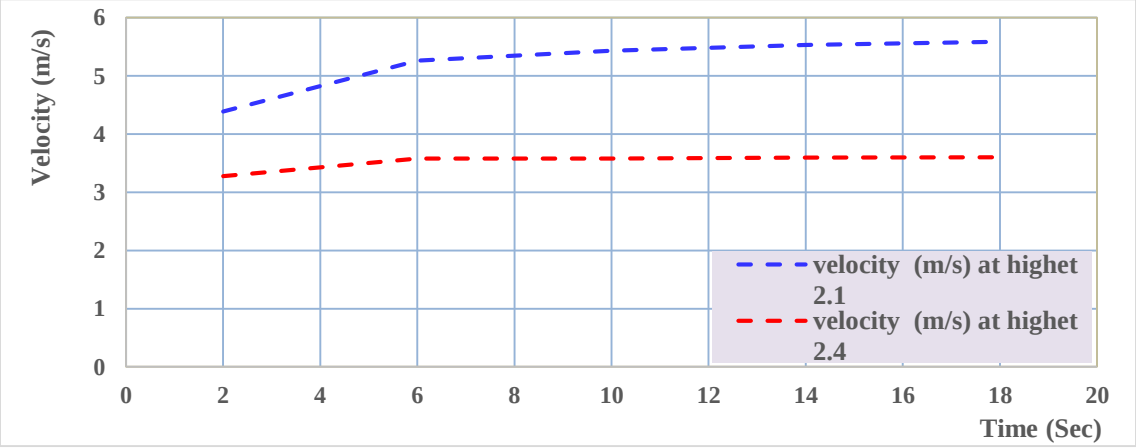

Figure 37. Comparison of all cases (velocity in point (3) in the velocity (2.5 m/s)).

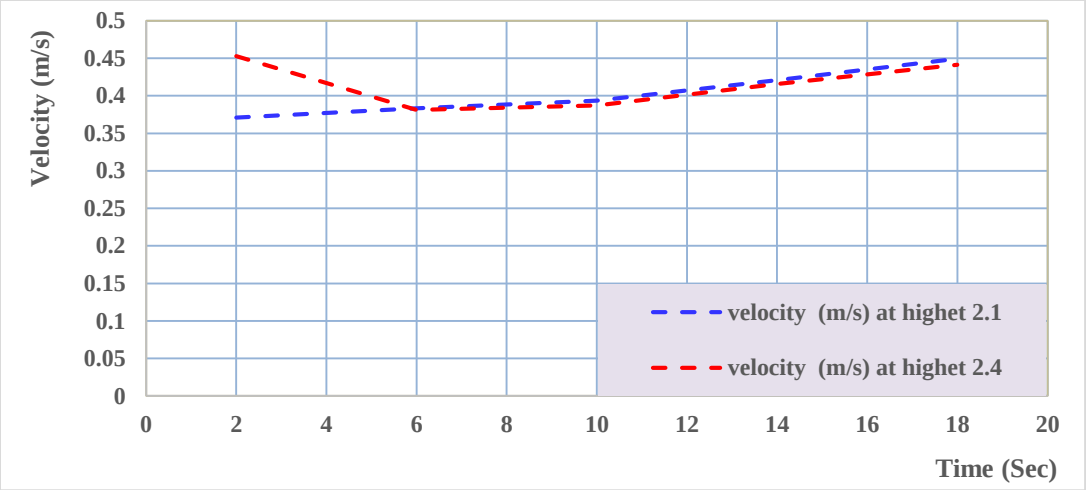

Figure 38. Comparison of all cases (velocity in point (3) in the velocity (6,5 m/s)).

4. Conclusions

This numerical study was conducted to investigate the effect of installation height of heating and cooling equipment on the distribution of temperature and airflow within an enclosed space. The simulations were performed using ANSYS/FLUENT 16. Two representative situations were taken into consideration, where in the first case, the device height was 2.1 m, and in the second case, it was 2.4 m high.

The findings indicate that the higher device location of the device (2.4 m) offers the best performance in the distribution of temperature and air velocity throughout the domain. This increased distribution directly affects the general quality of thermal comfort, with conditioned air penetrate in further into the space, and covering a large area, thus, reducing local temperature gradients. It was also noted that the higher the installation height, the faster the system transfers heat and thus it is more efficient in stabilizing indoor conditions.

These results are supported by quantitative comparisons. At point (1), the heat transfer at a speed of 2.5 m/s increased by 0.377 % when the device was raised by 2.1 to 2.4 m whereas at point (3) the rise was 0.288 %. At the higher velocity of 6.5 m/s, but only 0.227% at point (1) and 0.184% at point (3). These values may sound numerically insignificant but they clearly indicate that height, rather than velocity variations, has a stronger effect on heat transfer performance.

This observation highlights a significant practical implication, which is that not only would optimization of the vertical arrangement of heating and cooling systems lead to better indoor comfort but also promoting energy conservation. The system can therefore be used to distribute more efficiently, leading to a reduction in the amount of unnecessary energy use and maximizing the performance of building appliances and equipment.

5. Future Work

1) Expanded Parameter analysis: Analyze a wider range of cooling device heights, room dimensions, and heat loads to optimize performance.
2) Experimental Validation: Validate numerical results through physical experiments for practical applicability.
3) Energy Optimization: Develop models to integrate cooling height, airflow velocity, and energy consumption for efficiency.
4) Smart Systems Integration: Explore IoT-enabled systems for adaptive control and enhanced cooling performance.
5) Environmental Impact assessment: Evaluate energy savings and carbon emission reductions from optimal cooling device placement.

Declaration of competing interest

The authors declare that they have no known competing financial interests or personal relationships that could have appeared to influence the work reported in this paper.

Data availability

The data that support the findings of this study are available on request from the corresponding author.

Declaration of generative AI and AI-assisted technologies in the writing process

-None

Disclosures

The authors have no conflicts of interest to declare in relation to this report.

References

[1] Guven, S "Calculation of optimum insulation thickness of external walls in residential buildings by using exergetic life cycle cost assessment method: Case study for Turkey" Environ. Prog. Sustain. Energy, 38(6), pp. 1–10, 2019, doi: 10.1002/ep.13232.

[2] Gao, T, Sandberg, L.I.C., and Jelle, B.J. "Nano insulation materials: Synthesis and life cycle assessment" Procedia CIRP, 15, pp. 490–495, 2014, doi: 10.1016/j.procir.2014.06.041.

[3] Cao, X., Dai, X., and Liu, J. "Building energy-consumption status worldwide and the state-of-the-art technologies for zero-energy buildings during the past decade" Energy Build, 128, pp. 198–213, 2016, doi: 10.1016/j.enbuild.2016.06.089.

[4] Lee, G.H., Park, B.K., and Lee, W. "Microstructure and property characterization of flexible syntactic foam for insulation material via mold casting" Int. J. Precis. Eng. Manuf. - Green

Technol., 4(2), pp. 169–176, 2017, doi: 10.1007/s40684-017-0021-2.

[5] Morsy, M., Fahmy, M., Abd Elshakour, H., and Belal, A.M. "Effect of Thermal Insulation on Building Thermal Comfort and Energy Consumption in Egypt" J. Adv. Res. Appl. Mech. J., 43(1), pp. 8–19, 2018.

[6] Leng, G. *et al.* "Preparation and properties of polystyrene/silica fibres flexible thermal insulation materials by centrifugal spinning" Polymer (Guildf), 185, 2019, doi: 10.1016/j.polymer.2019.121964.

[7] Xue, X., Wu, H., Zhang, X., Dai, J. and Su, C. "Measuring energy consumption efficiency of the construction industry: The case of China" J. Clean. Prod., 107, pp. 509–515, 2015, doi: 10.1016/j.jclepro.2014.04.082.

[8] Akyüz, M.K., Altuntaş, Ö. , and Söğüt, M.Z. "Economic and environmental optimization of an airport terminal building's wall and roof insulation" Sustain., 9(10), 2017, doi: 10.3390/su9101849.

[9] Abu-Jdayil, B., Mourad, A.H., Hittini, W., Hassan, M., and Hameedi, S. "Traditional, state-of-the-art and renewable thermal building insulation materials: An overview" Constr. Build. Mater., 214, pp. 709–735, 2019, doi: 10.1016/j.conbuildmat.2019.04.102.

[10] Zhao, J. *et al.*, "Development of high thermal insulation and compressive strength BPP foams using mold-opening foam injection molding with in-situ fibrillated PTFE fibers" Eur. Polym. J., 98, pp. 1–10, 2018, doi: 10.1016/j.eurpolymj.2017.11.001.

[11] Nyers, J., Kajtar, L., Tomić, S., and Nyers, A."Investment-savings method for energy-economic optimization of external wall thermal insulation thickness" Energy Build., 86, pp. 268–274, 2015, doi: 10.1016/j.enbuild.2014.10.023.

[2] Adamczyk , J, and Dylewski, R. "The impact of thermal insulation investments on sustainability in the construction sector" Renew. Sustain. Energy Rev., 80, 2016, pp. 421–429, 2017, doi: 10.1016/j.rser.2017.05.173.

[13] Huang, H., *et al.*, "Optimum insulation thicknesses and energy conservation of building thermal insulation materials in Chinese zone of humid subtropical climate" Sustain. Cities Soc., 52, 2019, p. 101840, 2020, doi: 10.1016/j.scs.2019.101840.

[14] Tsalagkas, D., Börcsök, Z., and Pásztory, Z. "Thermal, physical and mechanical properties of surface overlaid bark-based insulation panels" Eur. J. Wood Wood Prod., 77(5), pp. 721–730, 2019, doi: 10.1007/s00107-019-01436-5.

[15] Zhang, C., Wang, J., Luo, X., Song, L., Li, J., and Feng, Z. "Experimentally measured effects of height and location of the vortex generator on flow and heat transfer characteristics of the flat-plate film cooling" Int. J. Heat Mass Transf., 141, pp. 995–1008, 2019, doi: 10.1016/j.ijheatmasstransfer.2019.07.042.

[16] Chen, Q., and Liu, X. "CFD analysis of air distribution and thermal comfort in mechanically ventilated rooms" Energy and Buildings, 285, 2023, 112883.

[17] Zhang, Y., Wang, S., and Jin, X. "Influence of air-supply device location on indoor airflow and temperature distribution" Applied Thermal Engineering, 238, 2024, 121987.

[18] Kong, X., et al. "Numerical investigation of jet-induced airflow and thermal stratification in confined spaces" Building and Environment, 239, 2023, 110394.

[19] Elsheikh, A. H., et al. "CFD-based optimization of HVAC operating parameters for energy-efficient buildings" Energy Conversion and Management, 301, 2024, 118147.

[20] Huang, L., and Chen, Z. "Recent advances in numerical modeling of indoor airflow and thermal comfort" Renewable and Sustainable Energy Reviews, 189, 2025, 114356.

[21] Ariyarathna, I.S., Abeyrathna, W.P., Danilina, N., and Halwatura, R.U. "Life cycle cost-based design of energy-efficient office buildings for sustainable urban transition in tropical cities" Urban Transitions, 5, 2026, 100026.

[22] Huang, P., Zheng, X., Zhang, Y., and Shen, P. "Space layout automation and optimization for energy-efficient buildings: A multi-objective evolutionary approach with machine learning analytics" Energy and Buildings, 358, 2026, 117213.

[23] Poosapadi, D., Devi, G.M., Padmapriya, G., Srinivasan, K., Logeshwaran, T., Rani, J.A., Kumar, C.R., kumar, E.R., and Khan, M.A. "Energy Efficient Smart Control Strategies: Applying Machine Learning to Enhance Efficiency in Eco-Friendly Building Management for Renewable Energy Systems" Sustainable Computing: Informatics and Systems, 50, 2026, 101315.

[24] Zhang, J., Rasdi, M.T.M., Zainordin, N., and Qin, Y. "A comprehensive review of advanced energy-efficient technologies for building envelopes: Focus on walls, windows, and roofs" Energy Reports, 15, 2026, 108981.

[25] Liu, K., Xu, X., Lin, D., Zhang, R., Zhao, L., Abuduwayiti, A., and Causone, F. "A scalable and efficient framework for city-scale building energy modeling with microclimate considerations" Sustainable Cities and Society, 138, 2026, 107187.

[26] Zhou, Z., Jia, B., Yuan, W., and Zhang, J. "An efficient hybrid prediction methodology for building vibrations near high-speed railway bridges with analysis of resultant vibrational energy transfer characteristics" Journal of Sound and Vibration, 630, 2026, 119714.

[27] Konhäuser, K. and Werner, T. "Uncovering the financial impact of energy-efficient building characteristics with eXplainable artificial intelligence" Applied Energy, 374, 2024, p. 123960. DOI: 10.1016/j.apenergy.2024.123960.

[28] Behr, S. M., Küçük, M., Neuhoff, K. (2023): "Energetische Sanierung von Gebäuden kann durch Mindeststandards und verbindliche Sanierungsziele beschleunigt werden". https://www.econstor.eu/handle/10419/272122.

[29] Sun, Y., Haghighat, F., and Benjamin C.M. "A review of the-state-of-the-art in datadriven approaches for building energy prediction" Energy and Buildings 221, 2020, p. 110022. DOI: 10.1016/j.enbuild.2020.110022.

[30] Werner, T., Konhäuser, K., and Schwarz, N. "Evaluating strategic retrofit measures for energy-efficient residential buildings with artificial intelligence" Energy and Buildings, 2026, 117205.

[31] Guo, X., Zhong, Y., Sui, Q., Gong, Ch., Zhai, C., Liu, B., Li, N., and Cai, G. "Dynamic photothermal modulation in energy-efficient buildings" Materials Today, 91, 2025, Pages 84-102.

[32] Zhang, C., Wang, J., Luo, X., Song, L., Li, J., and Feng, Z."Experimentally measured effects of height and location of the vortex generator on flow and heat transfer characteristics of the flat-plate film cooling" Int. J. Heat Mass Transf., 141, pp. 995–1008, 2019, doi: 10.1016/j.ijheatmasstransfer.2019.07.042.

التحليل العددي لتأثير ارتفاع جهاز التبريد على توزيع درجة الحرارة وتدفق الهواء في حيز مغلق

الخلاصة: تُسهم هذه الدراسة إسهامًا هامًا في سدّ الفجوة البحثية القائمة في الجهود المبذولة لتحقيق أقصى قدر من كفاءة الطاقة والراحة الحرارية في البيئات الداخلية، إذ تُقدّم تحليلًا عدديًا غير مستقر لتأثير ارتفاع جهاز التبريد على توزيع درجة الحرارة في حيز مغلق. وتستخدم الدراسة برنامج ANSYS FLUENT 16 لتقييم تأثير موقع الأجهزة على سرعة الهواء وتوزيع الحرارة. وتشير النتائج إلى أن ارتفاع 2.4 متر لجهاز التبريد أكثر فعالية من غيره في تحسين توزيع درجة الحرارة وسرعة الهواء. وقد وُجد أن زيادة ارتفاع الجهاز إلى 2.4 متر بسرعة 2.5 متر/ثانية تُحسّن انتقال الحرارة بنسبة 0.377% عند النقطة 1 و0.288% عند النقطة 3. وبالمثل، تبلغ الزيادة في انتقال الحرارة عند النقطتين 1 و3 بسرعة 6.5 متر/ثانية 0.227% و0.184% على التوالي. تُثبت هذه النتائج أن الارتفاع أكثر تأثيرًا على كفاءة نقل الحرارة مقارنةً بتكييف الهواء. تُسلط هذه الورقة الضوء على أهمية الموقع الاستراتيجي لأنظمة التبريد لتعزيز استخدامها الفعال والراحة الحرارية، مما يُسهم في التصميم والتشغيل المستدامين للمباني.

الكلمات المفتاحية: جهاز التبريد؛ توزيع درجة الحرارة؛ التحليل العددي؛ الانسز/فلونت.